OPEN ACCESS
Fractals (2025) 2540297 (12 pages)

DOI: 10.1142/S0218348X25402972

World Scientific
www.worldscientific.com

OPTICAL SOLITON SOLUTION OF THE BENNEY–ROSKES/ ZAKHAROV–RUBENCHIK SYSTEMS

MEHMET FATİH UÇAR
Department of Mathematics and Computer Science
Istanbul Kultur University
Istanbul, Turkey
f.ucar@iku.edu.tr

Received December 26, 2024
Accepted May 28, 2025
Published September 26, 2025

Abstract

The study focuses on deriving optical soliton solutions for the Benney–Roskes (BR) and Zakharov–Rubenchik (ZR) system. To achieve this, complex wave transformations are applied to convert the system of partial differential equations (PDEs) into a more manageable form of ordinary differential equation (ODE). This transformation simplifies the analysis and facilitates the extraction of exact solutions. The new Kudryashov method (nKM) is employed to solve the resulting nonlinear ODE (NODE). This powerful analytical technique allows for the derivation of various types of soliton solutions, including bright solitons, kink solitons, and singular solitons. Each type of soliton represents different physical phenomena and wave behaviors, providing a comprehensive understanding of the system's dynamics. The study includes the visualization of the obtained soliton solutions through graphical representations. These visualizations

help in understanding the spatial and temporal evolution of the solitons and their interaction with the medium. Furthermore, the study analyzes how changes in the system's parameters individually affect the shape, amplitude, and width of the solitons. This parametric analysis is crucial for predicting and controlling soliton behavior in practical applications. These are the main distinctive parts and novelties of this study. By deriving and analyzing soliton solutions, the study provides deeper insights into the nonlinear interactions within the BR and ZR system. Understanding these interactions is essential for applications in optical communications, where solitons can be used to transmit information over long distances without significant loss or distortion.

Keywords: Optical Solitons; Benney–Roskes System; Zakharov–Rubenchik System; The New Kudryashov Method; Parameter Effect.

1. INTRODUCTION

The study of nonlinear dynamics and wave interactions has been a central focus in the field of fluid mechanics and plasma physics, with the Benney–Roskes (BR) and Zakharov–Rubenchik (ZR) systems being two important models that have received significant attention from researchers. The BR and ZR system is a fundamental model in the study of nonlinear wave interactions, particularly in the context of water waves and plasma physics. This system describes the dynamics of weakly nonlinear waves, where the nonlinear effects are small compared to the linear wave dynamics. The BR system of equations was originally derived in the study of gravity waves by Benney and Roskes.[1] It describes the evolution of weakly nonlinear long waves in a stratified shear flow and has been used to study phenomena such as the emergence of solitary waves and the transfer of energy between different scales of motion.

This system is equivalent to the ZR system, whose derivation and physical basis are elaborated in Refs. 2–4. The ZR system, on the other hand, is a model for the interaction between surface and internal waves in a fluid with a variable bottom, and has been used to investigate the dynamics of waves in oceanographic and geophysical contexts.[5,6]

The exploration of the BR and ZR systems is of significant interest in the literature, particularly due to their implications in the study of wave dynamics in various media.[2,7] In this paper, we will investigate a $(2+1)$-dimensional BR and ZR system

$$\begin{aligned} &iU_t + aU_{xx} + \epsilon U_{yy} \\ &\quad = (b - wm)|U|^2 U \\ &\qquad - wU\left\{m\frac{\partial}{\partial t} + (mc - d)\frac{\partial}{\partial y}\right\}V, \\ &V_{xx} + (1 - mc^2)V_{yy} - mV_{tt} - 2mcV_{yt} \\ &\quad = \left\{m\frac{\partial}{\partial t} + (mc - d)\frac{\partial}{\partial y}\right\}|U|^2, \end{aligned} \tag{1}$$

where $U(x, y, t)$ denotes the complex-valued high frequency function and $V(x, y, t)$ denotes the real-valued hydrodynamic potential function. For the parameters, m represents the Mach number that is the ratio of the carrier wave's group velocity to the speed of sound, ϵ denotes a dispersion constant, d is associated with the Doppler shift, and w quantifies the coupling intensity with acoustic waves. The constants a and c are related to the group velocity, while the parameter b characterizes the self-interaction of the carrier wave. They are assumed to be nonzero real numbers throughout this analysis.

Passot *et al.* simplified the BR/ZR system by employing the Mach number and a rescaling approach.[7] They explored the influence of acoustic waves on the self-focusing behavior of high-frequency waves using the ZR systems. The simplification made the system more tractable for analysis, and the study of self-focusing behavior provided insights into how acoustic waves affect the concentration of energy in high-frequency waves. By further simplifying the universal BR/ZR system, the Davey–Stewartson system emerges. This system models the evolution of three-dimensional (3D) wave packets on water with finite depth.[8,9] Similarly, the Zakharov system can also be derived through analogous simplifications as introduced in Ref. 10, the Zakharov system explains Langmuir wave propagation in plasma. Haas' foundational work introduces the quantum Zakharov equations, which are the critical framework for understanding the interplay between quantum Langmuir waves and quantum ion-acoustic waves in electron-ion electrostatic quantum plasmas.[11] Danylenko *et al.*'s

study contributes to the understanding of chaotic regimes and the bifurcations that arise in complex media, thus enriching the discussion surrounding wave dynamics initiated by the quantum Zakharov framework.[12] Their work highlights how complex media can lead to chaotic behavior and bifurcations, which are critical for understanding the transition from ordered to disordered states in wave dynamics. Zhang *et al.* also explored the bifurcations and exact traveling wave solutions of the ZR equation.[13] Bifurcation analysis reveals how small changes in parameters can lead to qualitative changes in the system's behavior, while exact traveling wave solutions provide explicit examples of wave propagation. These results are valuable for understanding the stability and dynamics of wave solutions in the ZR system, with potential applications in nonlinear optics, plasma physics, and fluid dynamics. Ceballos gave the supersonic limit for the ZR system.[14] This work provides insights into the high-speed dynamics of the ZR system, which is relevant for applications in plasma physics and high-energy wave propagation. Dehghan *et al.* introduced the radial basis function partition of unity procedure combined with the reduced-order method for solving ZR equations.[15] The method is useful for simulating wave dynamics in complex media, enabling researchers to study phenomena that are difficult to analyze analytically. Similarly, Oruç introduced the radial basis function finite difference (RBF-FD) method for numerical simulation of interaction of high and low frequency waves for ZR equations[16] that enhances the ability to model and analyze wave interactions in nonlinear media, with applications in optics, acoustics, and plasma physics. Han *et al.* gave the chaotic behavior and traveling wave solutions of the fractional stochastic Zakharov system[17] that extends the classical Zakharov system to more realistic scenarios, providing insights into chaotic dynamics and wave propagation in stochastic and fractional media. Saut and Ponce reformulated the BR system as a nonlinear Schrödinger equation containing nonlocal terms and derivatives of the unknown, studying the local well-posedness of the Cauchy problem.[18] This reformulation allowed for the study of the local well-posedness of the Cauchy problem, ensuring that solutions exist, are unique, and depend continuously on initial data for a short time. Also Henao proposed the well-posedness and stability analysis of standing waves for a 1D-BR system.[19] This work confirmed that standing wave solutions are mathematically well-defined (well-posed) and analyzed their stability under small perturbations. Quintero and Cordero studied the nonlinear orbital instability of standing waves for the BR/ZR system in one and two spatial dimensions[20] that shows that small perturbations to standing wave solutions can grow over time, leading to significant deviations from the original solution. Gonul and Ozemir employed Lie symmetry analysis and traveling wave solutions of the system (1).[21,22] Lie symmetry analysis revealed symmetries of the system, which can simplify the equations or uncover new solutions. Traveling wave solutions are important for understanding wave propagation in nonlinear media.

The structure of the study is as follows: In Sec. 2, nonlinear ordinary differential equation (NODE) is derived from system (1). In Sec. 3, the method used is given briefly. In Sec. 4, results, visualization, and analyze of effect of parameters are discussed. Finally, in Sec. 5 conclusion is given.

2. DERIVATION OF THE NODE FORM OF THE SYSTEM (1)

To find the analytical solution of the system (1), we first consider a complex wave transform at form:

$$\begin{aligned} U(x,y,t) &= u(\xi)e^{i\Omega(x,y,t)}, V(x,y,t) = v(\xi) \\ \Omega(x,y,t) &= -kx + ly + nt + \phi_0, \\ \xi &= x + y - \alpha t, \end{aligned} \tag{2}$$

where $u(\xi)$ is the real-valued function that represents amplitude of the soliton and $v(\xi)$ is the real-valued hydrodynamic potential function. All other parameter values in (2) are real constants. Substituting (2) into system (1), we get the following first and second equations:

$$\begin{aligned} &(wm - b)u^3 + (a + \epsilon)u'' - (w + ak^2 + \epsilon l^2)u \\ &\quad = (wm\alpha - w(mc - d))uv' \end{aligned} \tag{3}$$

with the constraint equation from the imaginary part as

$$2l\epsilon - 2ak - \alpha = 0 \Rightarrow \alpha = 2ak - 2l\epsilon \tag{4}$$

and

$$\begin{aligned} &(2 - mc^2 - m\alpha^2 + 2mc\alpha)v'' \\ &\quad = 2(mc - m\alpha - d)uu', \end{aligned} \tag{5}$$

respectively. If we integrate Eq. (5) with respect to ξ and assume the integration constant as zero, we get

$$\begin{aligned} &(2 - mc^2 - m\alpha^2 + 2mc\alpha)v' \\ &\quad = (mc - m\alpha - d)u^2 \end{aligned} \tag{6}$$

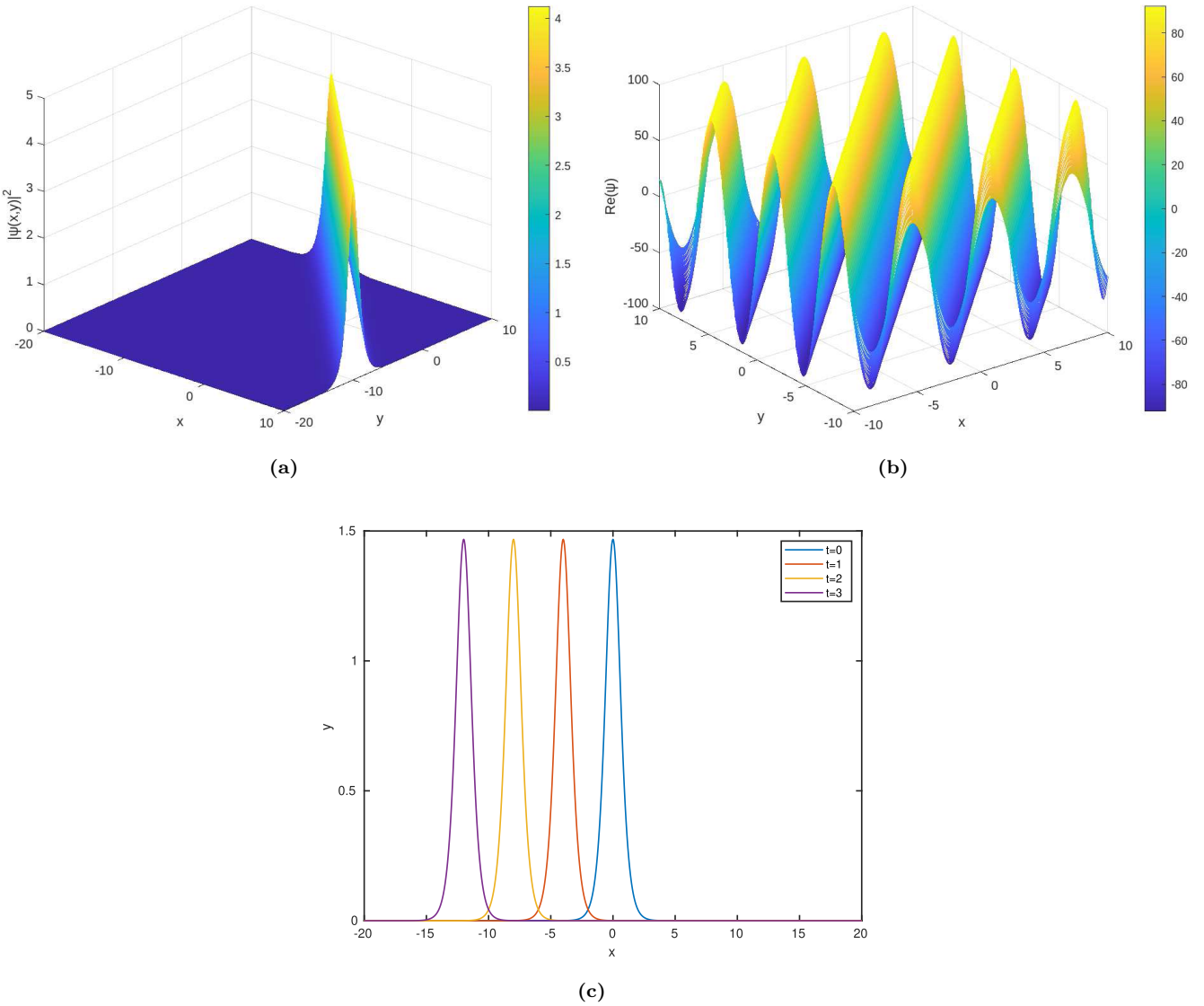

(a) **(b)** **(c)**

Fig. 1 The bright soliton depiction of Eq. (18). **(a)** 3D view of $|U_1(x,y,t)|^2$. **(b)** 3D view of $\Re(U_1(x,y,t))$. **(c)** 2D view of $|U_1(x,y,t)|^2$ for $t = 0, 1, 2$.

and so,

$$v' = \frac{mc - m\alpha - d}{2 - mc^2 - m\alpha^2 + 2mc\alpha} u^2 \tag{7}$$

provided that $2 - mc^2 - m\alpha^2 + 2mc\alpha = -2 + (\alpha - c)^2 m \neq 0$. If we substitute Eq. (7) into Eq. (3), we obtain the NODE

$$\begin{aligned} &((a+\epsilon)(-2+(\alpha-c)^2 m))u'' \\ &-((\alpha^2 b + (-2bc+2dw)\alpha \\ &-2wcd + bc^2 + 2w)m + wd^2 - 2b)u^3 \\ &+(ak^2 + \epsilon l^2 + n)(-2+(\alpha-c)^2 m))u = 0. \end{aligned} \tag{8}$$

In order to ascertain the balancing constant, the homogeneous balance principle is applied to Eq. (8). The balance of u^3 and u'' implies the relation $3N = N + 2$, which simplifies to $N = 1$.

3. THE NEW KUDRYASHOV METHOD AND ITS IMPLEMENTATION

We introduce the algorithms of the nKM in this section.[23,24] According to the nKM, the solution of Eq. (8) is given in the form

$$u(\xi) = \sum_{i=0}^{N=1} A_i R^i(\xi) = A_0 + A_1 R(\xi), \qquad A_1 \neq 0. \tag{9}$$

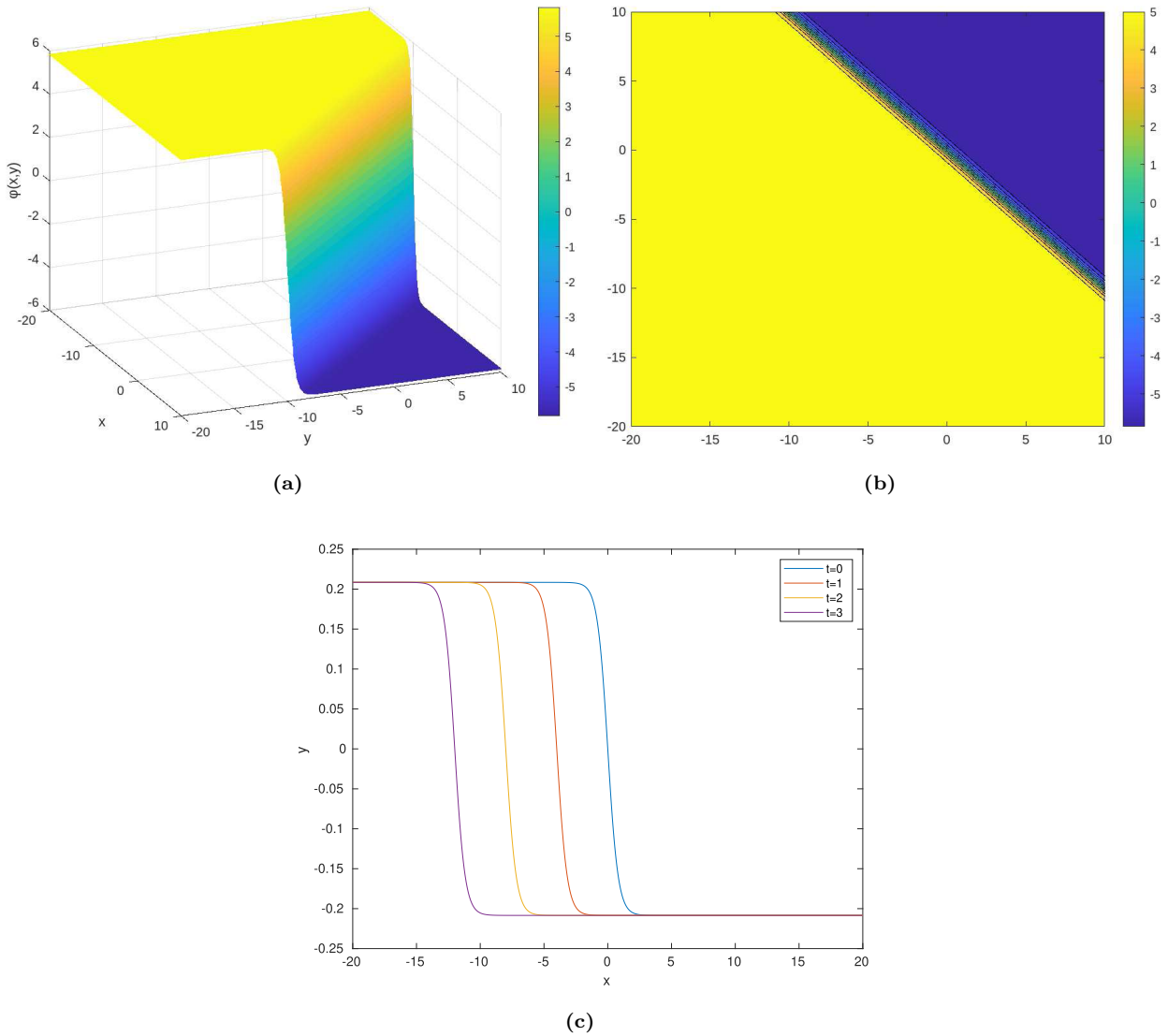

Fig. 2 The kink soliton depiction of Eq. (19). **(a)** 3D view of $V_1(x, y, 0)$, **(b)** Contour projection of $V_1(x, y, 0)$, **(c)** 2D view of $V_1(x, y, t)$ for $t = 0, 1, 2, 3$.

Here, $R(\xi)$ is the solution of the following differential equation:

$$\frac{dR(\xi)}{d\xi} = \sqrt{\delta^2 R^2(\xi)(1 - \eta\, R^2(\xi))}, \tag{10}$$

where δ, η are nonzero arbitrary real parameters. It can be written in the form

$$R(\xi) = \frac{4L}{4L^2 e^{\delta\xi} + \eta e^{-\delta\xi}}, \tag{11}$$

where L is a nonzero free parameter. Equation (11) can be shown in the hyperbolic form:

$$R(\xi) = \frac{4L}{(4L^2 + \eta)\cosh(\delta\xi) + (4L^2 - \eta)\sinh(\delta\xi)}. \tag{12}$$

Equations (11) and (12) result in the bright soliton when $\eta = 4L^2$ as

$$R(\xi) = \frac{1}{2L}\mathrm{sech}(\delta\xi), \tag{13}$$

and the singular soliton when $\eta = -4L^2$ as

$$R(\xi) = \frac{1}{2L}\mathrm{csch}(\delta\xi). \tag{14}$$

The application of Eqs. (9) to (8), utilizing the properties of Eq. (10), results in the following algebraic system of equations, which is derived from the coefficients of $R^j(\xi)$ for $0 \le j \le 3$:

$$\begin{aligned} R^0\colon\ & -4A_0((\epsilon^3 l^4 + l^2(k(k-2l)a + A_0^2 b + cl + n)\epsilon^2 \\ & -2(k^2(k - l/2)a^2 + k(A_0^2 b - 1/2ck \\ & +1/2cl + n)a - c^2 l/8 + ((-bc + dw)A_0^2)/2 \end{aligned}$$

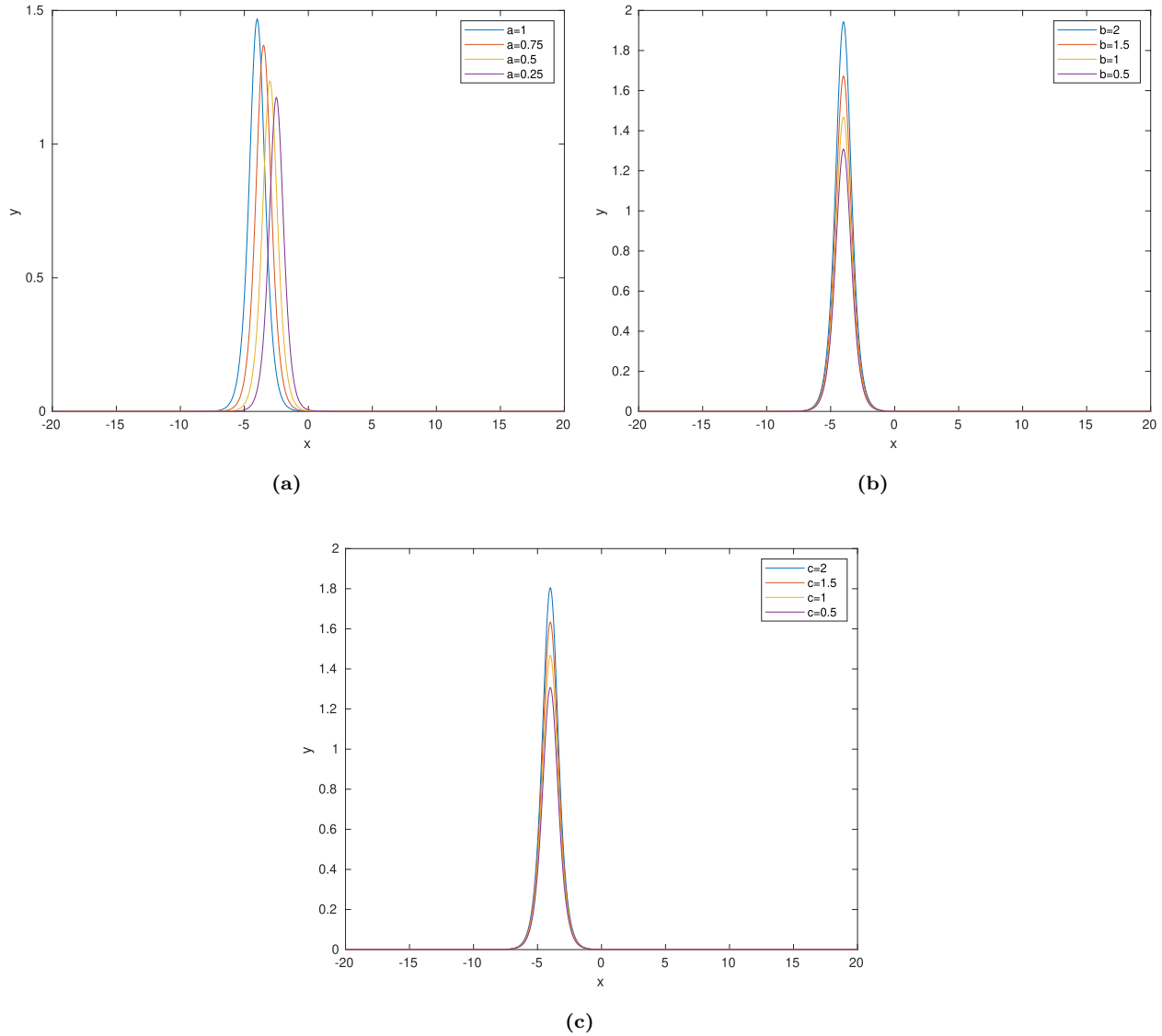

(a) **(b)** **(c)**

Fig. 3 The bright soliton type in Fig. 1 and the effect of the parameters a, b, c. **(a)** Effect of a, **(b)** Effect of b, **(c)** Effect of c.

$$
\begin{aligned}
&-cn/2)l\epsilon + a^3k^4 + k^2(bA_0^2 - ck + n)a^2\\
&-(-c^2k/4 + (bc - dw)A_0^2 + cn)ka\\
&+((-wcd + 1/2bc^2 + w)A_0^2)/2 + c^2n/4)m\\
&-\epsilon l^2/2 - ak^2/2 + ((wd^2/2 - b)A_0^2)/2\\
&-n/2) = 0,\\
R^1:\ &-4A_1(((-\delta^2l^2 + l^4)\epsilon^3 + l((k^2l + 2(\delta^2 - l^2)k\\
&-l\delta^2)a + cl^2 + (3bA_0^2 + n)l - c\delta^2)\epsilon^2\\
&+((-2k^3l + (-\delta^2 + l^2)k^2 + 2kl\delta^2)a^2 + (ck^2l\\
&+(-cl^2 + 2(-3bA_0^2 - n)l + c\delta^2)k - cl\delta^2)a\\
&+c^2l^2/4 + ((3bA_0^2 + n)c - 3dwA_0^2)l - c^2\delta^2/4)\epsilon\\
&+(-\delta^2k^2 + k^4)a^3 + (-ck^3 + (3bA_0^2 + n)k^2
\end{aligned}
\qquad
\begin{aligned}
&+ck\delta^2)a^2 + (c^2k^2/4 + ((-3bA_0^2 - n)c\\
&+3dwA_0^2)k - c^2\delta^2/4)a + ((3bA_0^2 + n)c^2)/4\\
&-(3A_0^2wcd)/2 + (3A_0^2w)/2)m + ((\delta^2 - l^2)\epsilon)/2\\
&+((\delta^2 - k^2)a)/2 + 3(wd^2/2 - b)A_0^2/2\\
&-n/2) = 0,\\
R^2:\ &-12A_0A_1^2(((ka - l\epsilon - c/2)^2b + w(adk - \epsilon dl\\
&-1/2cd + 1/2))m + wd^2/4 - b/2) = 0,\\
R^3:\ &-8A_1((\epsilon^3l^2\eta\delta^2 - 2(((k - l/2)a - c/2)\eta\delta^2\\
&-A_1^2bl/4)l\epsilon^2 + (((k - 2l)a - c/2)\eta(ka - c/2)\delta^2\\
&-l(abk + 1/2dw - 1/2bc)A_1^2)\epsilon\\
&+a\eta(ka - c/2)^2\delta^2 + ((bk^2a^2 + k(-bc + dw)a
\end{aligned}
$$

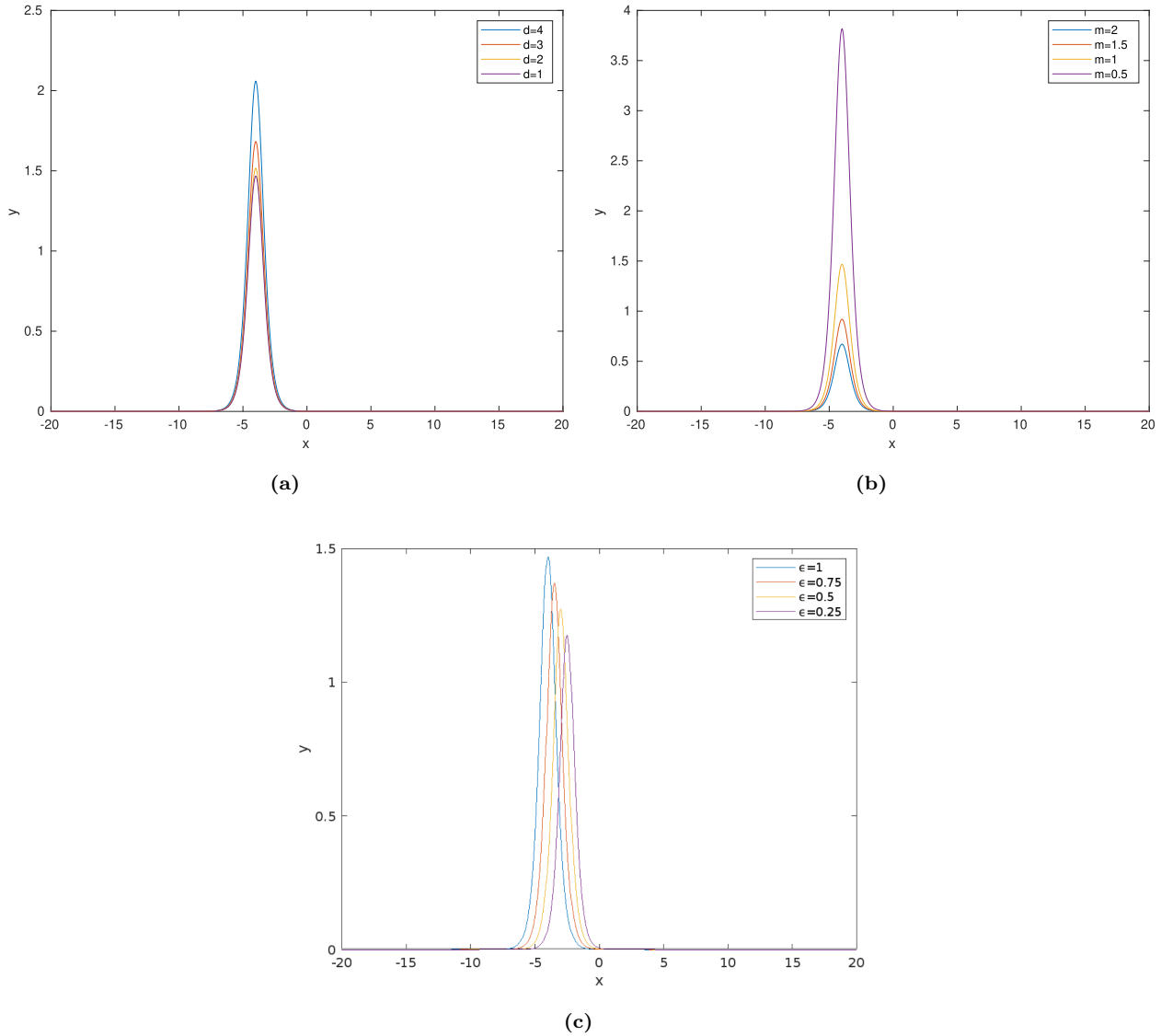

Fig. 4 The bright soliton type in Fig. 1 and the effect of the parameters d, m, ϵ. **(a)** Effect of d, **(b)** Effect of m, **(c)** Effect of ϵ.

$$
\begin{aligned}
&- wcd/2 + bc^2/4 + w/2)A_1^2)/2)m - \delta^2\epsilon\eta/2 \\
&- a\delta^2\eta/2 + A_1^2(d^2w - 2b)/8) = 0. \qquad (15)
\end{aligned}
$$

We derive the following solution sets using Maple 2023 symbolic calculation package:[25]

$$
\begin{aligned}
\delta &= \mp\sqrt{\frac{ak^2 + \epsilon l^2 + n}{a + \epsilon}} \\
A_1 &= \mp((4a^2bk^2m - 8ab\epsilon klm + 4b\epsilon^2l^2m - 4abckm \\
&\quad + 4adkmw + 4bc\epsilon lm - 4d\epsilon lmw + bc^2m \\
&\quad - 2cdmw + d^2w + 2mw - 2b)/(8a^3\eta k^4m \\
&\quad - 16a^2\epsilon\eta k^3lm + 8a^2\epsilon\eta k^2l^2m + 8a\epsilon^2\eta k^2l^2m \\
&\quad - 16a\epsilon^2\eta kl^3m + 8\epsilon^3\eta l^4m - 8a^2c\eta k^3m \\
&\quad + 8ac\epsilon\eta k^2lm - 8ac\epsilon\eta kl^2m + 8c\epsilon^2\eta l^3m \\
&\quad + 8a^2\eta k^2mn + 2ac^2\eta k^2m - 16a\epsilon\eta klmn \\
&\quad + 2c^2\epsilon\eta l^2m + 8\epsilon^2\eta l^2mn - 8ac\eta kmn \\
&\quad + 8c\epsilon\eta lmn + 2c^2\eta mn - 4a\eta k^2 \\
&\quad - 4\epsilon\eta l^2 - 4\eta n))^{1/2} \\
A_0 &= 0. \qquad (16)
\end{aligned}
$$

So, we gain the solution function of system (1) as

$$
U(x, y, t) = \frac{4A_1L * e^{i(-kx+ly+nt+\phi_0)}}{B}, \qquad (17)
$$

where

$$
B = 4L^2e^{\delta(x+y-(2ak-2l\epsilon)t)} + \eta e^{-\delta(x+y-(2ak-2l\epsilon)t)},
$$

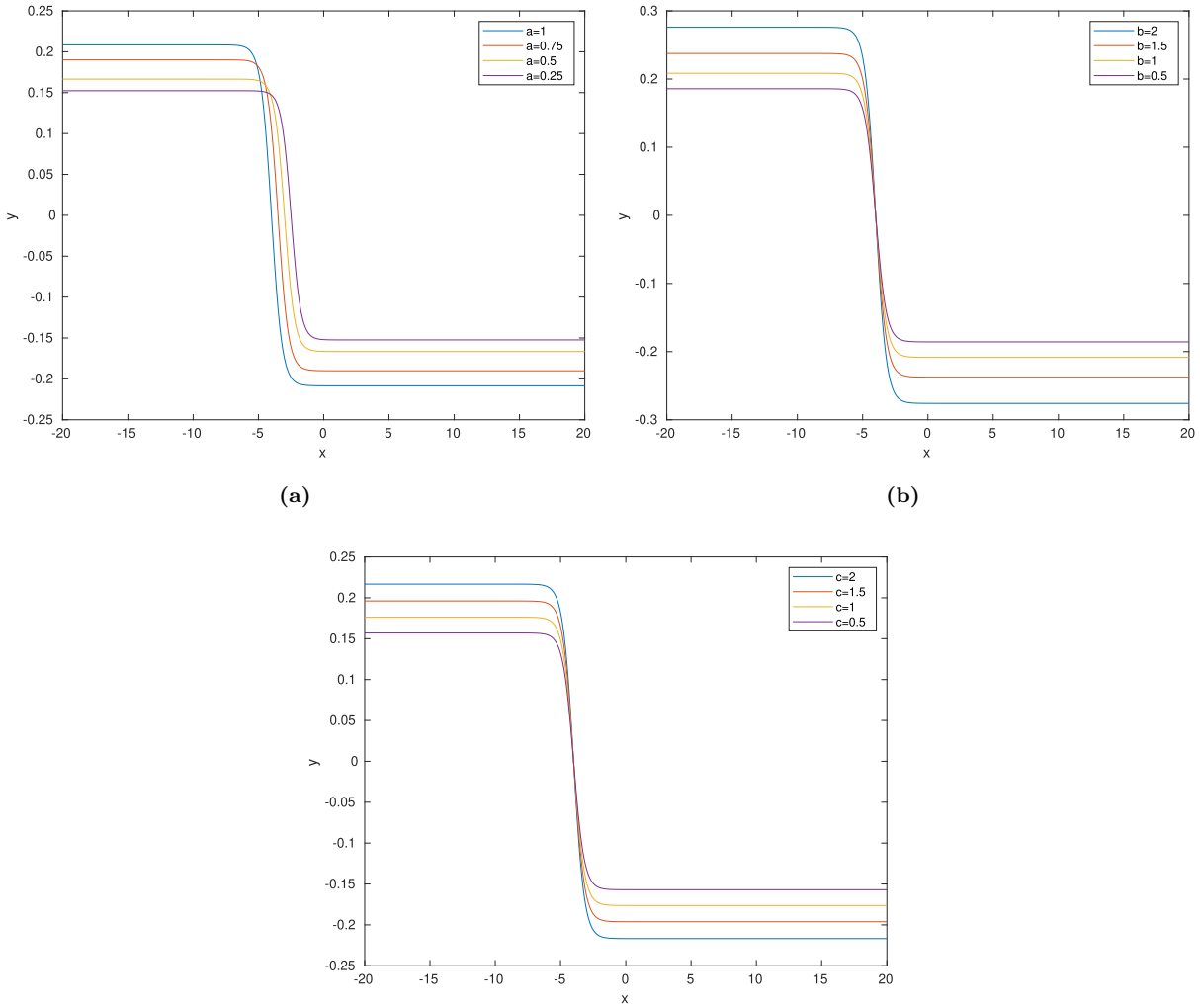

Fig. 5 The kink soliton type in Fig. 2 and the effect of the parameters a, b, c. **(a)** Effect of a, **(b)** Effect of b, **(c)** Effect of c.

δ and A_1 are presented in set (16). For $\eta = 4L^2$, Eq. (17) can be rewritten to yield the following structure, which gives the bright soliton:

$$U_1(x,y,t) = \frac{A_1}{2L}\text{sech}(\delta(x+y-(2ak-2l\epsilon)t)) \times e^{i(-kx+ly+nt+\phi_0)}, \tag{18}$$

and from Eq. (7) we get the kink soliton:

$$V_1(x,y,t) = \frac{A_1^2 D}{4L^2\delta}\tanh(\delta(x+y-(2ak-2l\epsilon)t)), \tag{19}$$

where

$$D = \frac{mc-m\alpha-d}{2-mc^2-m\alpha^2+2mc\alpha}, \quad \alpha = 2(ak-l\epsilon).$$

On the other hand, for $\eta = -4L^2$, Eq. (17) is transformed into the form, which represents the singular soliton pair:

$$U_2(x,y,t) = \frac{A_1}{2L}\text{csch}(\delta(x+y-(2ak-2l\epsilon)t)) \times e^{i(-kx+ly+nt+\phi_0)}, \tag{20}$$

$$V_2(x,y,t) = -\frac{A_1^2 B}{4L^2\delta}\coth(\delta(x+y-(2ak-2l\epsilon)t)), \tag{21}$$

But in this study, we will concentrate on the graphical representation of bright and kink soliton solutions and effect of their parameters.

4. RESULTS AND DISCUSSION

This section illustrates the graphical representations of the obtained solution functions and provides interpretations based on these visualizations. Before presenting the results derived from Eqs. (18)

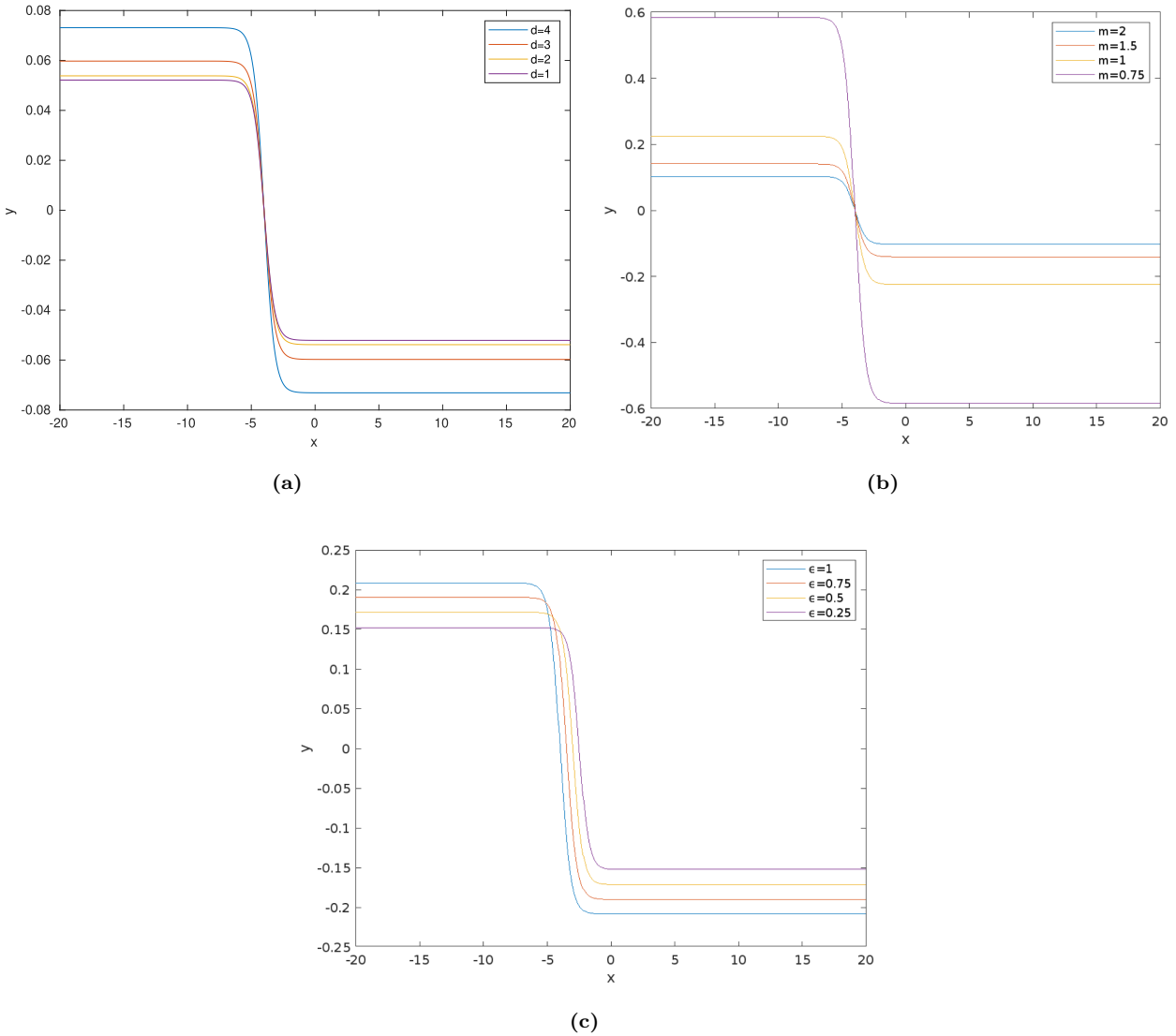

Fig. 6 The kink soliton type in Fig. 2 and the effect of the parameters d, m, ϵ. **(a)** Effect of d, **(b)** Effect of m, **(c)** Effect of ϵ.

and (19), it is crucial to ensure that these solutions satisfy the primary equation under investigation, represented by Eq. (1). Without this verification, the solutions and their corresponding graphs would lack significance.

Once it is confirmed that the solutions satisfy Eq. (1), the next step is to derive meaningful solitons by selecting suitable parameters. The solutions provided by Eqs. (18) and (19) were examined using the parameter set $a = 1$, $b = 1$, $m = 1$, $\epsilon = 1$, $n = 1$, $d = 1$, $c = 1$, $w = 3$, $k = -1$, $l = 1$, $\phi_0 = 0.5$. This parameter selection resulted in the bright soliton form shown in Fig. 1 and the kink soliton form illustrated in Fig. 2. It should be emphasized that these parameter values are not the only possible choices; other parameter configurations can also yield similar bright and kink soliton forms, provided a meaningful soliton solution is obtained. For instance, Fig. 1a depicts a 3D representation of the function $|U_1(x, y, 0)|^2$, showcasing a bright soliton. When observed along the x-axis, the right side covers a smaller flat region compared to the left skirt. Figure 1b displays a 3D plot of $Re(U_1(x, y, 0))$ with a periodic alpha structure, while Fig. 1c complements this with a contour representation. Furthermore, Fig. 1d presents a two-dimensional (2D) plot of $|U_1(x, y, t)|^2$ at $t = 0$ (blue), $t = 1$ (red), $t = 2$ (orange) and $t = 3$ (purple) that demonstrates the movement of the bright soliton to the leftover time.

Figure 2a presents a 3D visualization of the function $V_1(x, y, 0)$, illustrating a kink soliton. When observed along the x-axis, the soliton features an asymmetry, with a smaller flat region on the left

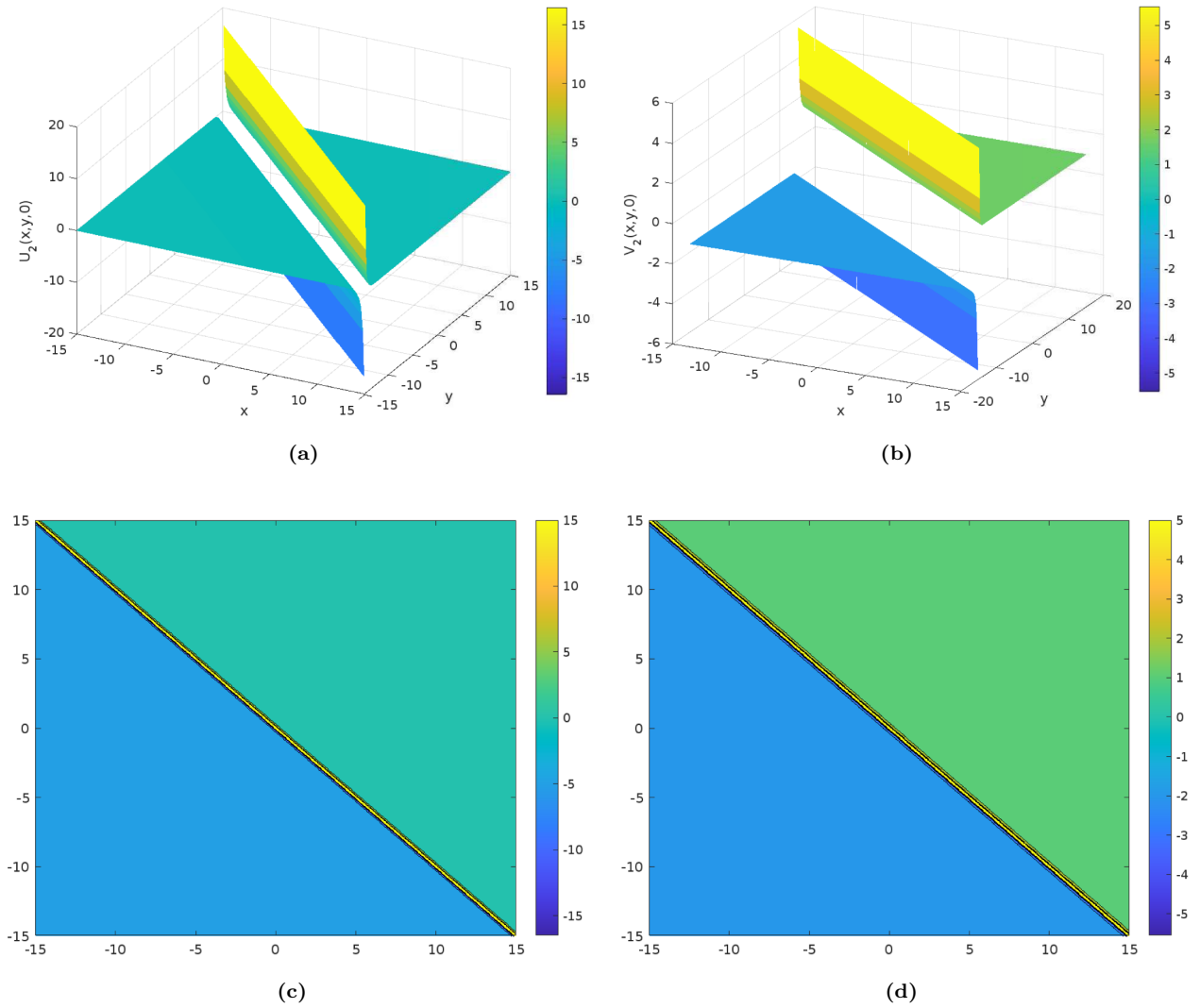

Fig. 7 The singular soliton depiction of Eqs. (20) and (21) **(a)** 3D view of $|U_2(x,y,t)|^2$, **(b)** 3D view of $V_2(x,y,t)$, **(c)** Contour projection of $Re(U_2(x,y,0)$, **(d)** Contour projection of $V_2(x,y,0)$.

compared to the extended upward region on the right. Figure 2b complements this depiction by providing a contour plot of the same function. Meanwhile, Fig. 2c showcases a 2D plot of $V_1(x,y,t)$ for various time instances: $t = 0$ (blue), $t = 1$ (red), $t = 2$ (orange), and $t = 3$ (purple). This plot reveals the leftward motion of the kink soliton over time.

Figures 3 and 4 explore the behavior of the $|U_1(x,y,1)|^2$ bright soliton under the influence of several parameters: m (Mach number), ϵ (dispersion constant), d (Doppler shift), and the group velocity parameters a and c. The self-interaction parameter b, associated with the carrier wave, is also examined. In Fig. 3a, the bright soliton's shape is plotted for different values of the group velocity parameter a ($a = 0.25, 0.5, 0.75, 1.00$). However, as a decreases, both the soliton's amplitude and its rightward movement diminish. Figure 3b examines the impact of the self-interaction parameter b with values $b = 0.5, 1.0, 1.5, 2.0$. Here, the amplitude of the bright soliton decreases as b is reduced. A similar trend is observed in Fig. 3c, where the parameter c is varied with identical values. In Fig. 4a, the influence of the Doppler shift parameter d ($d = 1, 2, 3, 4$) is depicted. As d increases, the soliton amplitude grows, although this increase is nonlinear compared to the linear increments of d. Figure 4b demonstrates the effect of the Mach number m, showing that soliton amplitude rises with m, again in a nonlinear fashion. Lastly, in Fig. 4c, the behavior of ϵ is analogous to that of a: as ϵ decreases, the soliton's amplitude and its rightward motion diminish, while its symmetry about a vertical axis through the peak remains intact.

Figure 5 explores the behavior of the kink soliton $V_1(x, y, 1)$ depicted in Fig. 2, considering the same parameters as in Figs. 3 and 4, at $t = 1$. To analyze this, Fig. 5a illustrates the kink soliton's form for varying values of the group velocity parameter a (0.25, 0.5, 0.75, and 1.00). It is evident from Fig. 5a that the soliton's amplitude diminishes as the value of a decreases, and the soliton appears to shift to the right with smaller a values. Figure 5b investigates the impact of the carrier wave's self-interaction parameter, using the same b values as in Fig. 3b. Similarly, the amplitude of the kink soliton decreases with lower b values.

In Fig. 5c, the behavior of another group velocity parameter, c, is examined using identical values to those in Fig. 3. The results mirror the trend observed for b. Likewise, Fig. 6a presents the effect of the Doppler shift parameter d, demonstrating behavior akin to b. However, unlike the bright soliton, the kink soliton's amplitude increases with rising d values. This increase, while evident, does not follow a linear trend, even though d itself increases linearly.

Figure 6b highlights an intriguing phenomenon: as the Mach number m decreases, the soliton's amplitude increases. However, this relationship also deviates from linearity. Lastly, the effect of the parameter ϵ shown in Fig. 6c resembles that of a. The soliton's amplitude decreases with smaller ϵ values, accompanied by an apparent rightward shift of the soliton form.

Figure 7 is the graphical representation of singular solitons $U_2(x, y, t)$ and $V_2(x, y, t)$ shown in Eqs. (20) and (21), respectively, but we will not analyze them in detail.

5. CONCLUSION

This research focuses on deriving soliton solutions for the BR and ZR systems using the new Kudryashov method. This study begins with the transformation of the system into a nonlinear ODE through a complex wave approach. Following this, various optical soliton solutions are obtained, including bright, kink, and singular soliton forms. The bright and kink solitons are illustrated in 3D, 2D, and contour representations. Furthermore, the impact of specific parameters on the obtained bright and kink soliton solutions is thoroughly analyzed. This study aims to deliver a comprehensive and straightforward understanding of these soliton solutions and their relevance in the field. Considering the advancements in modern communication and internet technologies and the pivotal role of fiber optic communication, this study highlights the significance of exploring different solution forms of the model. It also underscores the potential for expanding such investigations to encompass higher-order systems, providing valuable insights for researchers in this domain. It contributes to the broader field of nonlinear science by providing exact solutions and a detailed analysis of the ZR system. The results have potential applications in designing and optimizing systems that rely on nonlinear wave phenomena, such as fiber optics, water wave dynamics, and plasma wave interactions. For further studies, one may explore the influence of quantum or stochastic effects on the soliton dynamics in the ZR system, particularly in contexts where quantum fluctuations or noise play a significant role.

ORCID

Mehmet Fatih Uçar
https://orcid.org/0000-0002-5542-2222

REFERENCES

1. D. J. Benney and G. J. Roskes, Wave instabilities, *Stud. Appl. Math.* **48**(4) (1969) 377–385.
2. V. E. Zakharov, S. L. Musher and A. M. Rubenchik, Hamiltonian approach to the description of nonlinear plasma phenomena, *Phys. Rep.* **129**(5) (1985) 285–366.
3. V. E. Zakharov and E. A. Kuznetsov, Hamiltonian formalism for nonlinear waves, *Phys. Usp.* **40**(11) (1997) 1087–1116.
4. V. E. Zakharov and E. A. Kuznetsov, Solitons and collapses: two evolution scenarios of nonlinear wave systems, *Phys. Usp.* **55**(6) (2012) 535–556.
5. L. Fan, R. Liu and H. Gao, Hamiltonian model for coupled surface and internal waves over currents and uneven bottom, *Physica D* **443** (2023) 133558.
6. A. R. Osborne, Modeling the Davey–Stewartson (DS) equations, *Int. Geophys.* **97** (2010) 867–875.
7. T. Passot, C. Sulem and P. L. Sulem, Generation of acoustic fronts by focusing wave packets, *Physica D* **94**(4) (1996) 168–187.
8. A. Davey and K. Stewartson, On three-dimensional packets of surface waves, *Proc. R. Soc. Lond. A* **338**(1613) (1974) 101–110.
9. C. Klein and J.-C. Saut, Davey–Stewartson and related systems, in *Nonlinear Dispersive Equations: Inverse Scattering and PDE Methods* (Springer, 2022), pp. 215–316.
10. V. E. Zakharov, Collapse of Langmuir waves, *Sov. Phys. JETP* **35**(5) (1972) 908–914.

11. F. Haas, Variational approach for the quantum Zakharov system, *Phys. Plasmas* **14**(4) (2007) 042309.
12. V.A. Danylenko and S. I. Skurativskyi, Peculiarities of wave fields in nonlocal media, *Nonlinear Dynam. Syst. Theory* **16**(2) (2016) 165–178.
13. L. Zhang, P. Yuan, J. Fu and C. M. Khalique, Bifurcations and exact traveling wave solutions of the Zakharov–Rubenchik equation, *Discrete Contin. Dyn. Syst. Ser. S* **13**(10) (2020) 1–20.
14. J. C. Cordero Ceballos, Supersonic limit for the Zakharov–Rubenchik system, *J. Differ. Equ.* **261**(9) (2016) 5260–5288.
15. M. Dehghan, B. Hooshyarfarzin and M. Abbaszadeh, Radial basis function partition of unity procedure combined with the reduced-order method for solving Zakharov–Rubenchik equations, *Eng. Anal. Bound. Elem.* **145** (2022) 93–116.
16. Ö. Oruç, A radial basis function finite difference (RBF-FD) method for numerical simulation of interaction of high and low frequency waves: Zakharov–Rubenchik equations, *Appl. Math. Comput.* **394** (2021) 125787.
17. T. Han, C. Tang, K. Zhang and L. Zhao, Chaotic behavior and traveling wave solutions of the fractional stochastic Zakharov system with multiplicative noise in the Stratonovich sense, *Results Phys.* **48** (2023) 106404.
18. G. Ponce and J.-C. Saut, Well-posedness for the Benney–Roskes/Zakharov–Rubenchik system, *Discrete Contin. Dyn. Syst.* **13**(3) (2005) 811–825.
19. J. R. Q. Henao, On the well-posedness and stability analysis of standing waves for a 1D-Benney–Roskes system, *Tamkang J. Math.* **56**(2) (2025) 141–164.
20. J. R. Quintero and J. C. Cordero, Instability of the standing waves for a Benney–Roskes/Zakharov–Rubenchik system and blow-up for the Zakharov equations, *Discrete Contin. Dyn. Syst. Ser. B* **25**(4) (2020) 1213–1240.
21. Ş. Gönül and C. Özemir, Lie symmetries and traveling wave solutions of the 3D Benney–Roskes/Zakharov–Rubenchik system, *Chaos Solitons Fractals* **165** (2022) 112807.
22. Ş. Gönül and C. Özemir, Benney–Roskes/Zakharov–Rubenchik system: Lie symmetries and exact solutions, *Eur. Phys. J. Plus* **137**(10) (2022) 1107.
23. N. A. Kudryashov, Method for finding highly dispersive optical solitons of nonlinear differential equations, *Optik* **206** (2020) 163550.
24. M. Ozisik, A. Secer, M. Bayram and H. Aydin, An encyclopedia of Kudryashov's integrability approaches applicable to optoelectronic devices, *Optik* **265** (2022) 169499.
25. Maple, Version X *Maplesoft, a division of Waterloo Maple Inc.* Canada, https://www.maplesoft.com